

Type Ia supernova SN 2003du: optical observations

G.C. Anupama¹, D.K. Sahu^{1,2} and J. Jose^{1,2}

¹ Indian Institute of Astrophysics, II Block Koramangala, Bangalore 560 034, India
e-mail: gca@iiap.res.in

² Center for Research and Education in Science & Technology, Hosakote
e-mail: dks@crest.ernet.in

Received: 19/07/2004; accepted: 15/09/2004

Abstract. *UBVRI* photometry and optical spectra of type Ia supernova SN 2003du obtained at the Indian Astronomical Observatory for nearly a year since discovery are presented.

The apparent magnitude at maximum was $B = 13.53 \pm 0.02$ mag, and the colour $(B - V) = -0.08 \pm 0.03$ mag. The luminosity decline rate, $\Delta m_{15}(B) = 1.04 \pm 0.04$ mag indicates an absolute B magnitude at maximum of $M_B^{\max} = -19.34 \pm 0.3$ mag and the distance modulus to the parent galaxy as $\mu = 32.89 \pm 0.4$. The light curve shapes are similar, though not identical, to those of SNe 1998bu and 1990N, both of which had luminosity decline rates similar to that of SN 2003du and occurred in spiral galaxies. The peak bolometric luminosity indicates that $\sim 0.9 M_{\odot}$ mass of ^{56}Ni was ejected by the supernova. The spectral evolution and the evolution of the Si II and Ca II absorption velocities closely follows that of SN 1998bu, and in general, is within the scatter of the velocities observed in normal type Ia supernovae.

The spectroscopic and photometric behaviour of SN 2003du is quite typical for SNe Ia in spirals.

A high velocity absorption component in the Ca II (H & K) and IR-triplet features, with absorption velocities of $\sim 20\,000$ km s⁻¹ and $\sim 22\,000$ km s⁻¹ respectively, is detected in the pre-maximum spectra of days -11 and -7 .

Key words. supernovae: general - supernovae: individual: SN2003du

1. Introduction

The type Ia supernovae (SNe Ia) are widely believed to be the result of combustion of a degenerate white dwarf (Hoyle & Fowler 1960). The most likely models are: (1) an explosion of a CO white dwarf with a mass close to the Chandrasekhar limit, which accretes matter through Roche lobe overflow from an evolved companion star, (Whelan & Iben 1973) or (2) explosion of a rotating configuration formed from the merging of two low-mass white dwarfs, following the loss of angular momentum due to gravitational radiation (Webbink 1984; Iben & Tutukov 1984; Paczyński 1985; see Livio 2001 for a review). From the observed spectral and light curve properties, the first scenario appears to be the most likely candidate for a majority of SNe Ia. In both scenarios, a certain amount of material associated with the mass transfer is likely to remain in the system at the time of explosion. The interaction of the supernova with this material may lead to a shell structure in the ejecta (Khokhlov, Müller & Höflich 1993; Gerardy et al. 2004).

The temporal evolution of a supernova's luminosity contains important information on the physical pro-

cesses driving the explosion. The observed bolometric light curves provide a measure of the total output of converted radiation of SNe Ia, and hence serve as a crucial link to theoretical models of the explosion and evolution. The peak luminosity is directly linked to the amount of radioactive ^{56}Ni produced in the explosion (e.g. Arnett 1982, Höflich et al. 1996, Pinto & Eastman 2000) and can be used to test various explosion models.

A majority of SNe Ia belong to a fairly homogeneous class, in both their photometric as well as spectroscopic properties. While Branch et al. (1993) estimated 83% of the SNe Ia in their sample to be “normal” (SNe Ia that show conspicuous absorption features near 6150 Å due to Si II and near 3750 Å due to Ca II in their spectra near maximum light), a more recent study by Li et al. (2001) indicate 64% of SNe Ia are “normal”, 20% belong to the overluminous type similar to SN 1991T and 16% belong to the subluminous type similar to SN 1991bg. The peak absolute magnitudes of SNe Ia in the B , V , and R bands correlate with the decline rate of the immediate post-maximum light curve giving a photometric sequence from luminous blue events with relatively slow decline of the light curve to the subluminous red events with rapid decline of the light curve (e.g. Phillips 1993; Hamuy et al.

1996a; Hamuy et al. 1996b; Phillips et al. 1999). When arranged in the photometric sequence, SNe Ia also form a spectroscopic sequence (Branch et al. 1993). The peak absolute magnitude of SNe Ia is also correlated with the Hubble type of the parent galaxy. SNe Ia in ellipticals are, on an average, fainter than SNe Ia in spirals (Della Valle & Panagia 1992; Howell 2001). Although a majority of the SNe Ia are normal, some photometric and spectral inhomogeneities exist, even amongst these normal SNe Ia. The spectral variations are seen to correlate with the expansion velocity, the effective temperature and the peak luminosity (Nugent et al. 1995). The observed diversity indicate that SNe Ia cannot be described by a single parameter such as the early light curve decline and that the diversity is multidimensional (Hatano et al. 2000; Benetti et al. 2004). It is therefore important to study individual SNe events covering a wide spectral and temporal range.

We present in this paper the optical photometric and spectroscopic observations of the type Ia supernova SN 2003du. A description of the observations and analysis is given in Sec. 2, and the light and colour curves presented in Secs. 3 and 4. The absolute magnitude, the bolometric luminosity and the mass of ^{56}Ni ejected are discussed in Secs. 5 and 6. Section 7 gives a description of the spectral evolution, which is compared with other well studied normal SNe Ia.

2. Observations and Reduction

The supernova SN 2003du was discovered by Shwartz & Holvorcem (2003) on 2003 April 22.4, located 8.8 arcsec West and 13.5 arcsec South of the center of the nearby SBdm galaxy UGC 9391. Optical spectra by Kotak & Meilke (2003) obtained on April 24.06 indicated the supernova to be of type Ia, about two weeks before maximum. Based on a study of the spectra of SN 2003du during the early phases, Gerardy et al. (2004) report the detection of a high velocity component in the Ca II infrared triplet near 8000 Å. This feature exhibits a large expansion velocity, which is nearly constant between -7 and $+2$ days relative to maximum light and disappears shortly thereafter. Gerardy et al. (2004) suggest this feature can be caused by a dense shell formed when circumstellar material of solar abundance is overrun by the rapidly expanding outermost layers of the SN ejecta.

The observations of SN 2003du with the 2m Himalayan Chandra Telescope (HCT) at the Indian Astronomical Observatory (IAO), Hanle, India, began on 2003 April 24, two days after the discovery. The HFOSC instrument equipped with a SITE 2×4 K pixel CCD was used. The central 2×2 K region used for imaging corresponds to a field of view of $10 \text{ arcmin} \times 10 \text{ arcmin}$ at $0.296 \text{ arcsec pixel}^{-1}$. More details on the telescope and the instrument may be obtained from <http://www.iap.res.in/~iao>.

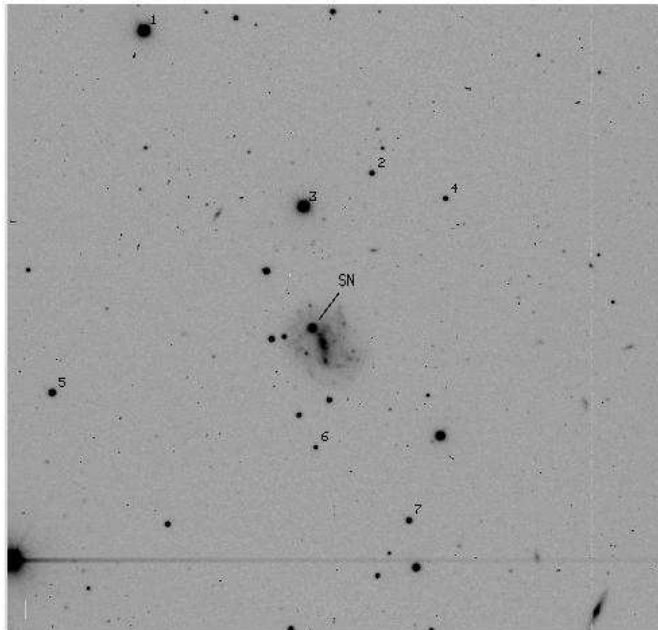


Fig. 1. Field of SN 2003du. The field of view is $10' \times 10'$. The stars used as local standards are listed in Table 1

2.1. Photometry

UBVRI photometry of SN 2003du were obtained during 24 April 2003 to 21 September 2003 and again in 2004, spanning $-12 - +362$ days since *B* maximum. The data were bias subtracted and flat field corrected in the standard manner using the various tasks under IRAF. Landolt (1992) standard regions PG0918+029, PG0942 - 029, SA101 (region covering stars 421, 338, 429, 431, 427, 341) and SA104 (region covering stars 330, 334, 336, 338, 339) were observed on 24 February 2004 and the regions PG0918+029, PG1047+003, PG1323 - 086, PG1530+057 were observed on 1 March 2004 under photometric conditions. These were used to estimate the atmospheric extinction and calibrate the field stars in the supernova region for use as secondary calibrators. They yield the following transformation equations:

$$\begin{aligned} u &= U - (0.188 \pm 0.02)(U - B) - (3.20 \pm 0.02) \\ b &= B - (-0.050 \pm 0.02)(B - V) - (1.01 \pm 0.003) \\ v &= V - (0.042 \pm 0.01)(B - V) - (0.634 \pm 0.003) \\ r &= R - (0.064 \pm 0.02)(V - R) - (0.721 \pm 0.01) \\ i &= I - (0.017 \pm 0.02)(V - I) - (1.01 \pm 0.01), \end{aligned}$$

where *ubvri* are the instrumental magnitudes corrected for atmospheric extinction and *UBVRI* are the standard magnitudes. The position of the supernova and the stars in the field used as local standards are shown marked in Fig. 1. Table 1 gives the magnitudes of the secondary standards, averaged over the two nights. These magnitudes were used to calibrate the data obtained on other nights.

Table 1. Magnitudes for the local sequence stars in the field of SN 2003du. The stars are identified in Fig. 1.

ID	U	B	V	R	I
1	13.80 ± 0.01	13.81 ± 0.02	13.19 ± 0.01	12.80 ± 0.003	12.43 ± 0.003
2	18.34 ± 0.01	17.67 ± 0.01	16.30 ± 0.01	15.31 ± 0.02	14.19 ± 0.02
3	13.85 ± 0.01	13.92 ± 0.02	13.37 ± 0.01	13.03 ± 0.01	12.72 ± 0.01
4	17.76 ± 0.02	18.04 ± 0.02	17.57 ± 0.01	17.22 ± 0.003	16.90 ± 0.02
5	16.53 ± 0.01	16.32 ± 0.03	15.58 ± 0.02	15.15 ± 0.01	14.74 ± 0.01
6	18.25 ± 0.04	18.67 ± 0.01	18.20 ± 0.01	17.86 ± 0.01	17.50 ± 0.01
7	17.14 ± 0.02	17.05 ± 0.02	16.33 ± 0.02	15.91 ± 0.01	15.51 ± 0.01

Table 3. Spectroscopic observations of SN 2003du

Date	J.D. 2400000+	Phase* (days)	Range Å
25/04/03	52755.5	-10.8	3500-7000; 5200-9200
29/04/03	52759.4	-6.9	3500-7000; 5200-9200
15/05/03	52775.3	+9.0	5200-9200
19/05/03	52779.4	+13.1	3500-7000; 5200-9200
12/06/03	52803.2	+36.9	3500-7000; 5200-9200
01/08/03	52853.2	+86.9	3500-7000; 5200-9200
21/09/03	52904.1	+137.8	3500-7000; 5200-9200
22/09/03	52905.1	+138.8	3500-7000; 5200-9200

* Relative to the epoch of B maximum JD = 2452766 .3

Aperture photometry was performed on the local standards using an aperture of radius 3-4 times that of the FWHM of the seeing profile that was determined based on an aperture growth curve. Since the underlying galaxy background at the location of the supernova is varying, the supernova magnitudes were obtained using the profile-fitting method, using a fitting radius corresponding to the FWHM of the seeing profile. The difference between aperture and profile-fitting magnitudes was obtained using the standards and this correction was applied to the supernova magnitude. The supernova magnitudes were calibrated differentially with respect to the local standards listed in Table 1. The estimated supernova magnitudes are listed in Table 2.

2.2. Spectroscopy

Spectroscopic observations of SN 2003du were made on eight occasions beginning 25 April 2003. The journal of observations is given in Table 3. All spectra were obtained at a resolution of ~ 7 Å in the wavelength range 3500-7000 Å and 5200-9200 Å. The one-dimensional spectra were extracted from the bias subtracted and flat-field corrected images using the optimal extraction method. Wavelength calibration was effected using the spectra of FeAr and FeNe sources. The wavelength calibrated spectra were corrected for instrumental response using spectra of spectrophotometric standards observed on the same night and brought to a flux scale. The flux calibrated spectra in the two different regions were combined, scaled to a weighted mean, to give the final spectrum on a relative flux scale.

3. The $UBVRI$ light curves

The $UBVRI$ light curves of SN 2003du are presented in Figs. 2a-e. Based on a cubic-spline fit to the points around maximum, it is estimated that the supernova reached a maximum B magnitude of 13.53 ± 0.02 mag on JD 245 2766.3 ± 0.5. Following Phillips (1993), we measure $\Delta m_{15}(B) = 1.04 \pm 0.03$. The main photometric parameters based on the light curves are listed in Table 4. The V maximum occurred later than the B maximum, while the maxima in U and I occurred ~ 1 day earlier, and the maximum in R coincided with the B maximum. The I light curve shows a secondary maximum ~ 25 d after B maximum at a magnitude ~ 0.5 mag fainter than the first maximum, similar to ‘normal’ SNe Ia (see e.g. Salvo et al. 2001). A noticeable rise in the R band is also seen at similar times, although coverage in our data at that period is poor.

We discuss in the following the light curve in each bandpass. The light curves in each bandpass are plotted individually, together with the light curves of other well observed type Ia SNe: SN 1994D (Richmond et al. 1995), SN 1990N (Lira et al. 1998), SN 1998bu (Suntzeff et al. 1999) and SN 1991T (Lira et al. 1998). All light curves are plotted such that the individual peak brightness is scaled with respect to that of its respective maximum (see Figs. 3a-e). The parameter $\Delta m_{15}(B)$ for each of these SNe are $\Delta m_{15}(B) = 1.26$ (SN 1994D: Patat et al. 1996), $\Delta m_{15}(B) = 1.03$ (SN 1990N: Lira et al. 1998), $\Delta m_{15}(B) = 1.01$ (SN 1998bu: Suntzeff et al. 1999) and $\Delta m_{15}(B) = 0.95$ (SN 1991T: Lira et al. 1998).

The U band light curve (Fig. 3a) indicates that SN 2003du is broader than SN 1994D, but narrower than SN 1991T. The light curve of SN 2003du is however very similar to those of SN 1990N and SN 1998bu. A similar trend is seen in the B band also (Fig. 3b). SN 2003du rises to maximum slower than SN 1994D, but faster than SN 1991T. The width of peak at 0.6 mag below maximum for SN1991T is about 21 days, for SN1994D is about 16 days and for SN2003du is about 20 days, similar to that of SN 1990N. Although differences are seen in the early decline, the decline rate of $1.45 \text{ mag } (100)^{-1}$ seen in SN 2003du at later phases is similar to that seen in SN 1991T and SN 1990N (Lira et al. 1998).

The V band light curve of SN2003du follows the same trend as that in the U and B bands. The early decline is slower than SN 1994D, but faster than SN 1991T. The

Table 2. Photometric observations of SN 2003du

Date	J.D. 2400000+	Phase* (days)	U	B	V	R	I	seeing (")
24/4/03	52754.2	-12.1	15.08 ± 0.03	15.30 ± 0.02	15.32 ± 0.02	15.22 ± 0.01	15.30 ± 0.02	1.7
25/4/03	52755.3	-11.0	14.55 ± 0.02	14.82 ± 0.02	14.91 ± 0.02	14.75 ± 0.02	14.77 ± 0.03	2.0
29/4/03	52759.3	-7.0	13.44 ± 0.03	13.94 ± 0.02	14.06 ± 0.02		14.29 ± 0.02	1.5
04/5/03	52764.2	-2.1	13.07 ± 0.03	13.55 ± 0.02	13.64 ± 0.02	13.62 ± 0.01	13.85 ± 0.02	2.1
09/5/03	52769.3	+3.0	13.25 ± 0.02	13.60 ± 0.02	13.63 ± 0.01	13.66 ± 0.01	14.04 ± 0.02	1.9
11/5/03	52771.3	+5.0	13.44 ± 0.02	13.72 ± 0.02		13.73 ± 0.01	14.13 ± 0.01	1.8
15/5/03	52775.2	+8.9	13.64 ± 0.02	13.97 ± 0.02	13.84 ± 0.01	13.90 ± 0.01	14.38 ± 0.01	1.7
18/5/03	52778.3	+12.0	14.01 ± 0.02	14.22 ± 0.02	14.00 ± 0.02	14.17 ± 0.01	14.57 ± 0.02	1.6
19/5/03	52779.3	+13.0	14.14 ± 0.02	14.35 ± 0.02	14.08 ± 0.02	14.23 ± 0.01	14.60 ± 0.01	1.6
25/5/03	52784.3	+18.0	14.76 ± 0.02	14.90 ± 0.02	14.36 ± 0.01	14.40 ± 0.01	14.59 ± 0.01	2.0
31/5/03	52791.4	+25.1	15.59 ± 0.02	15.65 ± 0.02	14.71 ± 0.01			1.9
01/6/03	52792.3	+26.0	15.68 ± 0.03	15.74 ± 0.02	14.74 ± 0.02	14.51 ± 0.01	14.42 ± 0.01	1.4
23/6/03	52814.2	+47.9			15.72 ± 0.03	15.49 ± 0.01	15.27 ± 0.03	2.4
28/6/03	52819.3	+53.0	16.72 ± 0.02	16.79 ± 0.02	15.90 ± 0.02	15.70 ± 0.02		3.0
03/7/03	52824.1	+57.8	16.85 ± 0.02	16.94 ± 0.02	16.05 ± 0.01	15.92 ± 0.02		2.0
01/8/03	52853.2	+86.9	17.49 ± 0.02	17.34 ± 0.02	16.79 ± 0.01	16.75 ± 0.02	16.95 ± 0.02	1.2
06/8/03	52858.2	+91.9		17.46 ± 0.02	16.91 ± 0.01	16.90 ± 0.01	17.12 ± 0.01	1.9
30/8/03	52882.2	+115.9		17.87 ± 0.02	17.51 ± 0.02	17.61 ± 0.02	17.95 ± 0.02	1.7
05/9/03	52888.1	+121.8		17.95 ± 0.03	17.60 ± 0.01	17.75 ± 0.02	18.03 ± 0.02	2.1
20/9/03	52903.1	+136.8	18.71 ± 0.04	18.10 ± 0.03	17.90 ± 0.03	18.05 ± 0.03		1.6
21/9/03	52904.2	+137.9		18.16 ± 0.02	17.94 ± 0.02	18.06 ± 0.02	18.14 ± 0.05	1.9
24/2/04	53060.5	+293.7		20.37 ± 0.05	20.32 ± 0.04	20.65 ± 0.06	19.90 ± 0.07	1.8
01/3/04	53066.5	+300.2		20.43 ± 0.04	20.24 ± 0.05	20.68 ± 0.10	19.88 ± 0.11	2.3
14/4/04	53110.5	+344.2				20.70 ± 0.06		1.9
02/5/04	53128.3	+362.0			20.77 ± 0.04	20.66 ± 0.06		2.0

* Relative to the epoch of B maximum JD = 2452766.3**Table 4.** Photometric parameters of SN 2003du

Data	U	B	V	R	I
epoch of max*	765.0 ± 1.0	766.3 ± 0.5	767.3 ± 0.5	766.6 ± 0.5	764.4 ± 0.5
magnitude at max	13.06 ± 0.03	13.53 ± 0.02	13.61 ± 0.02	13.61 ± 0.02	13.85 ± 0.02
early decline rate [†]	12.0	10.6	4.5		
decline rate days 100-300 ^{†,+}		1.45	1.51	1.66	1.07
$\Delta m_{15}(B)$		1.04 ± 0.03			
colours at B max		$U - B$	$B - V$	$V - R$	$R - I$
		-0.47 ± 0.04	-0.085 ± 0.03	-0.017 ± 0.03	-0.274 ± 0.03

* JD 2452000+

† mag (100d)⁻¹

+ Days since B maximum

shoulder that is seen close to 25 days after B maximum in the light curves of SN 1991T and SN 1998bu is not seen clearly in the light curve of SN2003du mainly due to the paucity of observation during that period.

A secondary peak characterizes the light curves of all normal and overluminous type SNe Ia, in both the R and I bands. The R band light curve is similar to SN 1998bu until the secondary maximum. Subsequently, the decline appears slower than that of SN 1998bu. In the I band, the light curve of SN 2003du is similar to that of SN 1998bu until the onset of the secondary maximum. Although the period around the secondary maximum is not well covered by our data, it appears that the day of secondary maximum (since B maximum) in SN 2003du is similar

to that of SN 1991T. Also, the decline from day 50-100 since B maximum follows that of SN 1991T rather than SN 1998bu. It is interesting to note here that the decline until the onset of the secondary maximum in SN 1990N closely matches that of SN 1991T.

From the light curves of SN 2003du in different filters and the estimate of $\Delta m_{15}(B)$ it is evident that SN 2003du differs significantly from normal SNe Ia occurring in ellipticals (like SN 1994D), being more similar to SN 1990N or SN 1998bu which occurred in spirals.

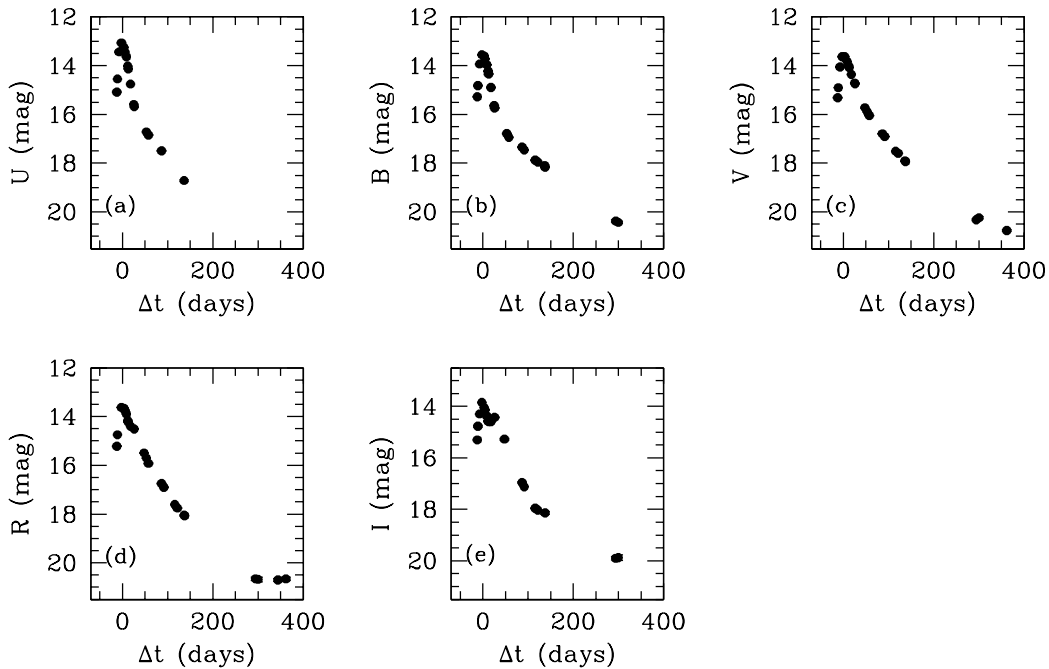


Fig. 2. The $UBVRI$ light curves of SN 2003du. The abscissae correspond to days since B maximum. The errorbars in magnitude are less than or comparable to the point size.

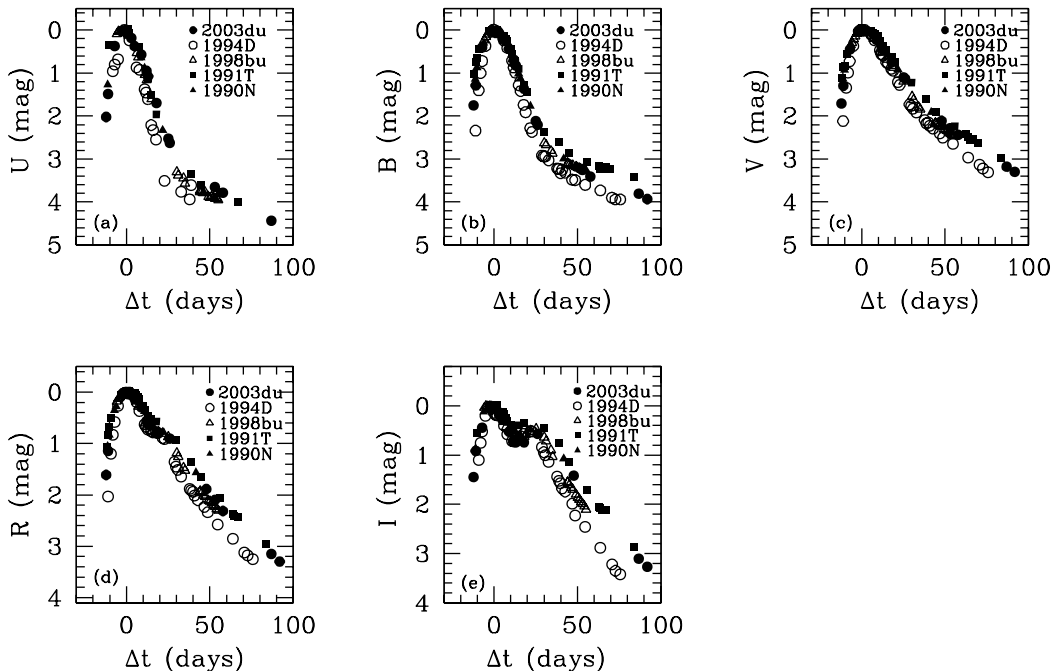


Fig. 3. U , B , V , R and I light curves of SNe 2003du, 1991T, 1990N, 1998bu and 1994D. The ordinate in each panel is the magnitude below the respective maximum, and the abscissae represent the days since respective B maximum

4. The colour curves

The dereddened $(U - B)$, $(B - V)$, $(V - R)$, and $(R - I)$ colour curves for SN 2003du are presented in Figs. 4a-d, together with those of SN 1991T, SN 1990N, SN 1998bu and SN 1994D. SN 2003du is corrected only for the Galactic reddening of $E(B - V) = 0.01$ (Schelgel et al.

1998), and the host galaxy extinction is assumed to be zero (refer to next section). The colours of the SNe Ia used here for comparison were reddening corrected using the Cardelli et al (1989) extinction law and the $E(B - V)$ values of $E(B - V) = 0.13$ for SN 1991T (Phillips et al. 1992), $E(B - V) = 0.32$ for SN 1998bu (Hernandez et al.

2000), $E(B-V) = 0.04$ (Richmond et al. 1995). SN 1990N has been corrected using only the Galactic reddening value of $E(B-V) = 0.026$ (Schelgel et al. 1998).

The $(U-B)$ colour (Fig. 4a) of SN 2003du is significantly different from that of SN 1994D, while the overall trend matches those of SNe SN 1991T, SN 1990N and SN 1998bu. At 12 days before B maximum, the $(U-B)$ colour of SN 2003du is about -0.2 , and gets bluer, reaching a value of -0.47 ± 0.03 mag at B maximum. This value compares well with that of the type Ia SN 1996X (Salvo et al. 2001). SN 2003du is redder compared to SN 1991T and SN 1998bu before and at B maximum. Subsequently, it remains bluer than SN 1991T, SN 1998bu and SN 1990N.

The $(B-V)$ colour (Fig. 4b) of SN 2003du follows the general trend of the colour curves of other type Ia supernovae. At 12 days before B maximum, the $(B-V)$ colour of SN 2003du is -0.05 mag, which gets bluer, reaching minimum -0.13 mag at 7 days before B maximum. At B maximum, $(B-V)$ is -0.08 mag, which is consistent with the intrinsic colours at maximum observed in other SNe Ia, which are in the range $\approx -0.1 - +0.1$ mag. Similar to the other SNe Ia SN 2003du attains $(B-V) = 1$ mag ~ 30 days after the B maximum, and thereafter the colour gets bluer. During pre-maximum to 15 days after B maximum phase, SN 2003du is bluer than the other supernovae in comparison, subsequently the $(B-V)$ colour compares well with SN 1991T.

As in the case of the $(U-B)$ and $(B-V)$ colour curves, the $(V-R)$ (Fig. 4c) colour curve of SN 2003du also evolves in a manner similar to other SNe Ia. While some differences are seen in the pre-maximum $(V-R)$ evolution of SN 2003du and SN 1991T, the evolution of the $(V-R)$ evolution of SN 2003du after the B maximum is very similar to that of SN 1991T. The $(V-R)$ colour is bluest at -0.17 mag 12 days past B maximum, and reaches 0.22 mag between 25–45 days after the B maximum.

The $(R-I)$ (Fig. 4d) colour evolution of SN 2003du is very similar to that of SN 1991T and generally bluer than the other SNe Ia being compared here. The $(R-I)$ colour reaches its bluest value of -0.5 mag around 10 days since B maximum, and subsequently gets increasingly redder. At later phases, (beyond day 50), both SN 2003du and SN 1991T are redder than the other SNe Ia.

5. The absolute magnitude of SN 2003du

The absolute magnitude of SN 2003du can be derived from the distance to the host galaxy or using the relation between the light curve shape and the SN absolute magnitude.

The reddening due to extinction within the host galaxy may be estimated either using the $(B-V)$ colour at maximum light, or using the $(B-V)$ colour during the decline, at a reference point of $t_V = 53$, where t_V is the phase measured in days since V maximum (Phillips et al. 1999). The observed $(B-V)$ at maximum (given $(B-V)_{\text{max}} = 0.07$; Phillips et al. 1999) suggests a reddening which is virtu-

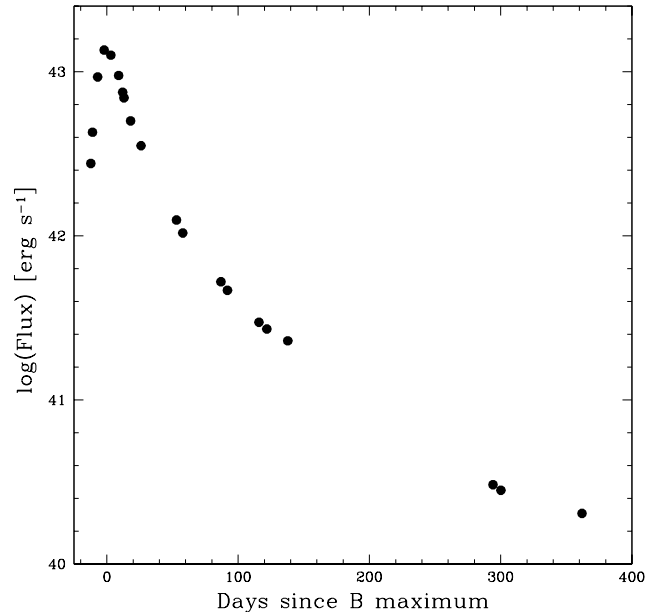


Fig. 5. The bolometric light curve of SN 2003du.

ally zero, while the observed $(B-V)$ colour at $t_V = 53$ gives a reddening estimate of $E(B-V) = 0.07 \pm 0.05$. Based on these estimates, we assume zero reddening due to the host galaxy, a result also confirmed by the absence of the Na I D absorption features in the spectra.

Using the relation between M_B versus $\Delta m_{15}(B)$ to calibrate the SN absolute magnitude, we obtain $M_B^{\text{max}} = -19.30 \pm 0.2$ (Hamuy et al. 1996a) and $M_B^{\text{max}} = -19.31 \pm 0.2$ (Phillips et al. 1999). Both methods give the same value for the absolute magnitude, which corresponds to a distance modulus of $\mu = 32.83 \pm 0.2$. Della Valle et al. (1998) give an improved estimate to the intercept in the Hamuy et al. (1996a) relation, using which we obtain $M_B^{\text{max}} = -19.42 \pm 0.3$ and $\mu = 32.95 \pm 0.3$. In the following, we use the average distance modulus of $\mu = 32.89 \pm 0.4$.

6. The bolometric light curve

The bolometric light curve of SN 2003du is estimated using the optical observations presented here, integrating the flux emitted in the U , B , V , R and I passbands. During the early phase, only the days on which data were available in all passbands were used. However, for the late phase (beyond day 90), we have integrated only over the available passbands. Contardo et al. (2000) have shown that the errors due to missing passbands in the optical do not exceed 10%. The bolometric light curve for a distance modulus $\mu = 32.89$, using only the optical data presented here indicates a peak at $\log L = 43.06$.

Combining the ultraviolet and near-IR data with the optical data for SN 1992A, Suntzeff (1996) has computed the *uvoir* bolometric luminosity, which integrates the flux emitted in the range 2000 Å– 2.2 μm . The ultraviolet flux contributes about 10 percent (maximum) to the to-

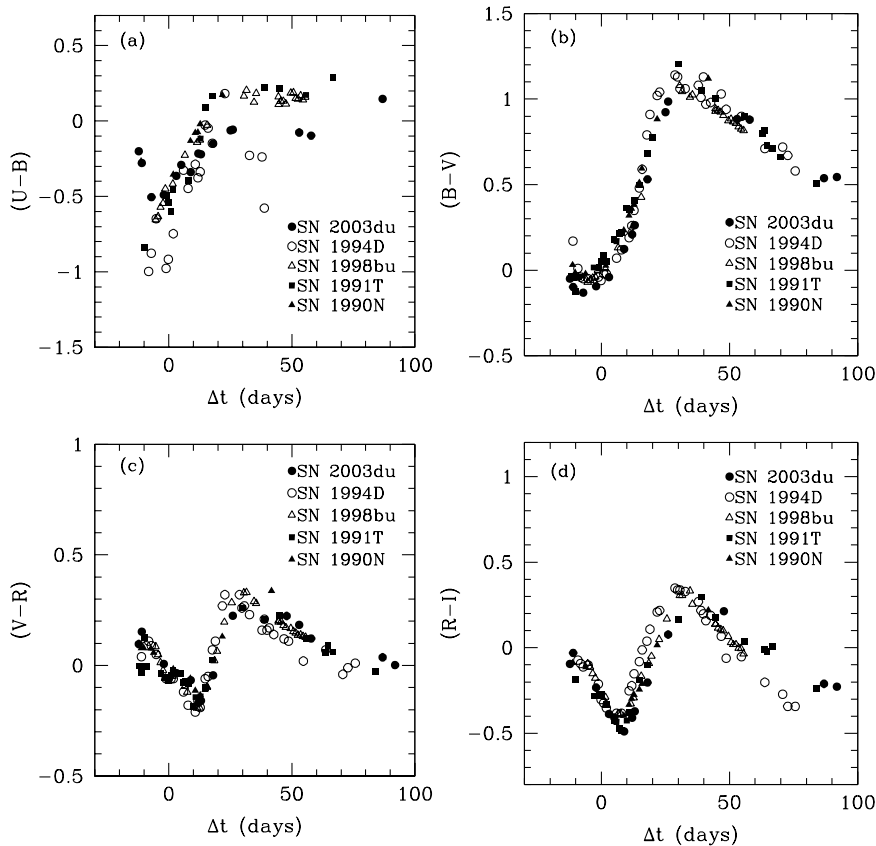


Fig. 4. The $U - B$, $B - V$, $V - R$ and $R - I$ colour curves of SN 2003du. Also shown for a comparison are the colour curves of SNe 1991T, 1990N, 1998bu and 1994D. The abscissae correspond to days since respective B maximum.

tal *voir* luminosity, while the near-IR contribution is also a maximum of 10-15 percent of the total *voir* luminosity for over ~ 80 days since B maximum. Thus, although the maximum contribution to the *voir* luminosity comes from the optical data, a correction is required to be applied the bolometric luminosity estimated using the optical data alone. Adopting a constant, total contribution of 20 percent from both ultraviolet and the near-IR regions, the *voir* luminosity estimated here indicates a peak luminosity of $\log L = 43.14$. The time evolution of the *voir* bolometric luminosity is presented in Fig. 5.

The amount of ^{56}Ni mass ejected may be estimated using the peak luminosity (Arnett 1982). Assuming the rise time of SN 2003du to be ~ 18 days and using the luminosity obtained by the optical data alone, the amount of ^{56}Ni ejected is estimated to be $0.73 M_{\odot}$. Using the corrected bolometric luminosity, the ^{56}Ni mass estimate is $0.88 M_{\odot}$.

7. The spectral evolution

Spectra of SN 2003du have been obtained at 4 epochs, from phase -11 to $+139$. They are presented in Figs. 6, 7 and 8. The early spectra are characterized by the deep absorption trough around 6000 \AA , due to Si II, typical of “normal” SNe Ia.

The spectral evolution of SN 2003du is similar to that of other SNe Ia, such as SN 1998bu (Jha et al. 1999), SN 1990N (Leibundgut et al. 1991), SN 1996X (Salvo et al. 2001) and SN 1994D (Patat et al. 1996). At early phases, the continuum is blue and dominated by lines due to the Fe-group and intermediate mass elements – Si, Ca, S, Mg. All lines exhibit the characteristic P-Cygni profiles, with the absorption shifting towards longer wavelengths, indicating a decrease in the expansion velocities with time. However, it is also possible that we are observing different layers that are moving at different velocities. The spectra at the later phases indicate a redder continuum, with nebular lines due to [Fe II] and [Fe III], which get dominant with time.

A more detailed comparison shows that although the spectra of all SNe Ia are similar, there are some differences in the detailed shapes and velocities of the features. For instance, in the early phase, the Ca II (H & K) feature in SN 2003du is stronger than in other SNe Ia being compared here. A similar strength of the Ca II (H & K) feature is seen in the -7 d spectrum of SN 1990N also (Leibundgut et al. 1991). In Fig. 9, we plot the -7 d spectrum of both SN 2003du and SN 1990N. The similarity between the two SNe is remarkable. The strength of the

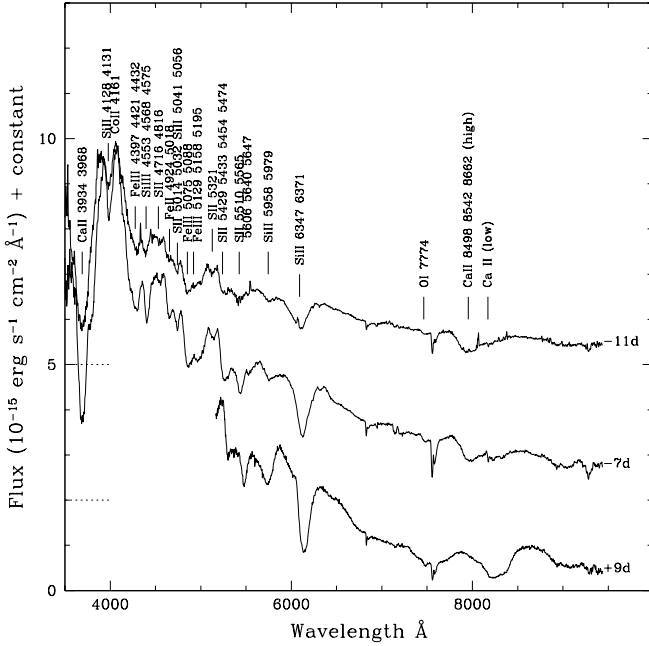


Fig. 6. The spectral evolution of SN 2003du from phase -11 d to $+9$ d. The spectra are not corrected for reddening. For clarity, the spectra have been displaced vertically. Dotted lines at the left indicate the zero flux level for each spectrum. For $+9$ d, zero flux is the x -axis. Wavelength scale is in the observer rest frame. Main line identifications are marked according to Mazzali et al. (1993).

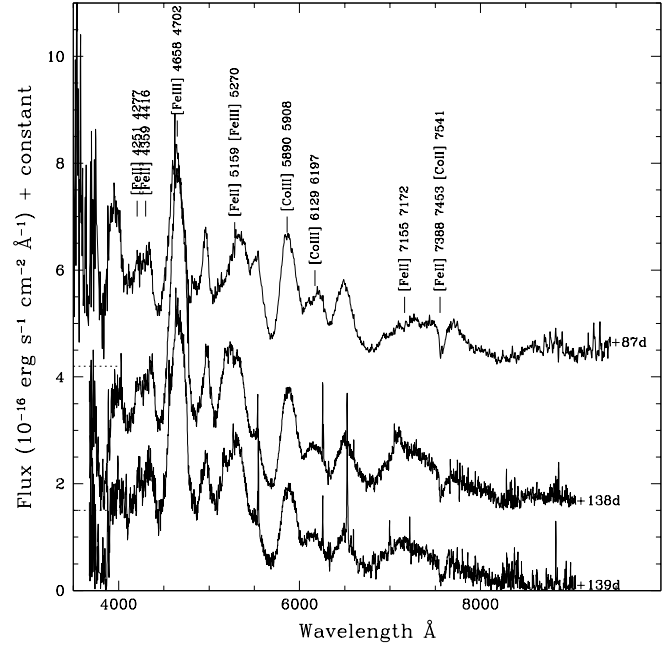


Fig. 8. The spectral evolution of SN 2003du from phase $+87$ d to $+139$ d. The spectra are not corrected for reddening. For clarity, the spectra have been displaced vertically. Dotted lines at the left indicate the zero flux level for each spectrum. For $+139$ d, zero flux is the x -axis. Wavelength scale is in the observer rest frame. Main line identifications are marked according to Bowers et al. (1997).

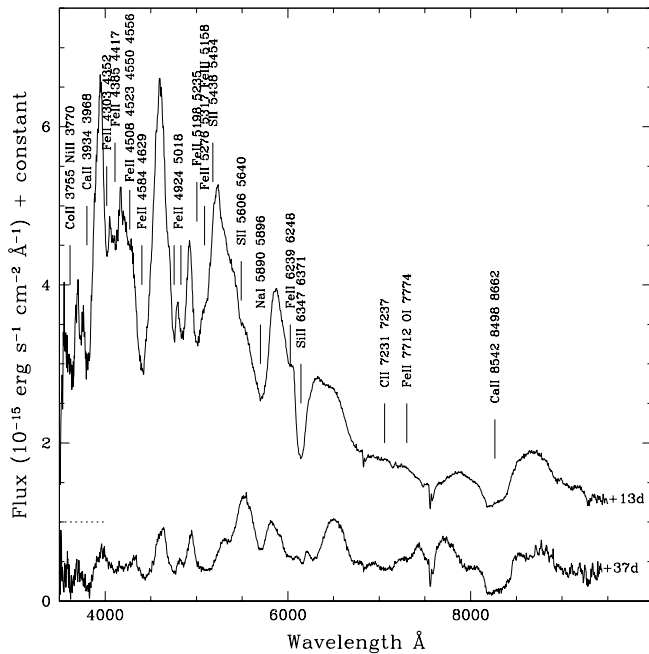


Fig. 7. The spectral evolution of SN 2003du from phase $+13$ d to $+37$ d. The spectra are not corrected for reddening. For clarity, the spectrum of $+13$ d has been displaced vertically and the dotted line at the left indicates the zero flux level. The zero flux for $+37$ d is the x -axis. Wavelength scale is in the observer rest frame. Main line identifications are marked according to Mazzali et al. (1993).

OI 7774 Å feature in SN 2003du is also more compared to the other SNe.

The high velocity absorption component of the Ca II infrared triplet detected by Gerardy et al. (2004) in the spectra of SN 2003du between day -5 to day $+2$ is seen in the spectra of days -11 and -7 presented here. This high velocity component is detected in the Ca II (H & K) absorption also. The low velocity component of the Ca II features appeared weakly on day -7 . While it is clearly detected in the IR triplet feature, it appears as a slight inflexion in the (H & K) feature. A similar inflexion is seen in the day -7 spectrum of SN 1990N also (see Fig. 9). The high velocity component disappeared by day $+6$. Gerardy et al. (2004) attribute this high velocity component as being caused by a dense shell formed when circumstellar material is overrun by the rapidly expanding outermost layers of the SN ejecta.

A quantitative comparison of the Si II 6355 Å and the Ca II (H&K) feature absorption velocities between SN 2003du and other typical SNe Ia: SN 1994D (Patat et al. 1996), SN 1998bu (Jha et al. 1999), SN 1996X (Salvo et al. 2001) and SN 1990N (Leibundgut et al. 1991) is illustrated in Fig. 10. From the Figure, it is seen that the velocities of the Si II feature in the pre-maximum phase in SN 2003du is lower than that of SN 1994D, but very similar to that of SN 1998bu and SN 1990N. A similar trend is seen in the high velocity component of the Ca II (H & K) absorption. The evolution of the absorption

- Branch, D., Fisher, A., Nugent, P. 1993, *AJ*, 106, 2383
- Bowers, E.J.C., Meikle, W.P.S., Geballe, T.R., et al. 1997, *MNRAS*, 290, 663
- Cardelli, J.A., Clayton, G.C., Mathis, J.S., 1989, *ApJ*, 345, 245
- Contardo, G., Leibundgut, B., Vacca, W.D., 2000, *A&A*, 359, 876
- Gerardy, C.L., Hoflich, P., Fesen, R.A., et al. 2004, *ApJ*, 607, 391
- Della Valle, M., Panagia, N., 1992, *AJ*, 104, 696
- Della Valle, M., Kissler-Patig, M., Danziger, J., et al. 1998, *MNRAS*, 299, 267
- Hamuy, M., Phillips, M.M., Schommer, R.A., et al. 1996a, *AJ*, 112, 2391
- Hamuy, M., Phillips, M.M., Suntzeff, N.B., et al. 1996b, *AJ*, 112, 2438
- Hatano, K., Branch, D., Lentz, E.J., et al. 2000, *ApJ*, L49
- Hernandez, M., Meikle, W.P.S., Aparicio, A., et al. 2000, *MNRAS*, 319, 223
- Höflich, P., Khokhlov, A., Wheeler, J.C., et al. 1996, *ApJ*, 472, L81
- Howell, D.A., 2001, *ApJ*, 554, L193
- Hoyle, F., Fowler, W.A., 1960, *ApJ*, 132, 565
- Jha, S., Garnavich, P.M., Kirshner, R.P., et al., 1999, *ApJS*, 125, 73
- Iben, I., Jr., Tutukov, A. V., 1984, *ApJS*, 54, 335
- Khokhlov, A., Müller, E., Höflich, P., 1993, *A&A*, 270, 223
- Kotak, R., Meilke, W.P.S., Rodriguez-Gil, P., 2003, *IAU Circ.* 8122
- Landolt, A.U., 1992, *AJ*, 104, 340
- Leibundgut, B., Kitshner, R.P., Filippenko, A.V., et al. 1991, *ApJ*, 371, 23
- Lira, P., Hamuy, M., Wells, L.A., et al. 1998, *AJ*, 115, 234
- Li, W., Filippenko, A., Treffers, R.R., et al. 2001, *ApJ*, 546, 734
- Livio, M., 2001 in *Space Telescope Science Institute Symposium Series Vol. 13, Supernova and Gamma Ray Bursts: The Greatest Explosions Since the Big Bang*, eds. M. Livio, N. Panagia & K. Sahu (Cambridge:Cambridge Univ. Press), 334
- Mazzali, P.A., Lucy, L.B., Danziger, I.J., et al. 1993, *A&A*, 269, 423
- Nugent, P., Phillips, M., Baron, E., et al. 1995, *ApJ*, 455, L147
- Paczynski, B., 1985 in *Cataclysmic Variables and Low-Mass X-Ray Binaries*, eds. D. Q. Lamb & J. Patterson (Dordrecht:Reidel), 1
- Patat, F., Benetti, S., Cappellaro, E., et al. 1996, *MNRAS*, 278, 111
- Phillips, M.M., 1993, *ApJ*, 413, L105
- Phillips, M.M., Wells, L.A., Suntzeff, N.B., et al. 1992, *AJ*, 103, 1632
- Phillips, M.M., Lira, P., Suntzeff, N.B., et al. 1999, *AJ*, 118, 1766
- Pinto, P.A., Eastman, R.G., 2000, *ApJ*, 530, 744
- Richmond, M.W., Treffers, R.R., Filippenko, A.V. et al. 1995, *AJ*, 109, 2121
- Salvo, M.E., Cappellaro, E., Mazzali, P.A., et al. 2001, *MNRAS*, 321, 254
- Schegel, D.J., Finkbeiner, D.P., Davis, M., 1998, *ApJ*, 500, 525
- Shwartz M., Holvorcem, P.R., 2003, *IAU Circ.* 8121
- Suntzeff, N.B., 1996, in *IAU Colloq. 145, Supernovae and Supernovae Remnants*, eds. R. McCray & Z. Wang (Cambridge: Cambridge Univ. Press), 41
- Suntzeff, N.B., Phillips, M.M., Covarrubias, R., et al. 1999, *AJ*, 117, 1175
- Webbink, R. F., 1984, *ApJ*, 277, 355
- Whelan, J., Iben, I., Jr., 1973, *ApJ*, 186, 1007